J|A|C|S ARTICLES

Published on Web 05/13/2010

Nanostructured Liquid Crystals Combining Ionic and Electronic Functions

Sanami Yazaki,[†] Masahiro Funahashi,*[,†] Junko Kagimoto,[‡] Hiroyuki Ohno,[‡] and Takashi Kato*[,†]

Department of Chemistry and Biotechnology, School of Engineering, The University of Tokyo, Hongo, Bunkyo-ku, Tokyo 113-8656, Japan, and Department of Biotechnology, Tokyo University of Agriculture and Technology, Nakacho, Koganei, Tokyo 184-8588, Japan

Received February 16, 2010; E-mail: funahashi@chembio.t.u-tokyo.ac.jp; kato@chiral.t.u-tokyo.ac.jp

Abstract: New molecular materials combining ionic and electronic functions have been prepared by using liquid crystals consisting of terthiophene-based mesogens and terminal imidazolium groups. These liquid crystals show thermotropic smectic A phases. Nanosegregation of the π-conjugated mesogens and the ionic imidazolium moieties leads to the formation of layered liquid-crystalline (LC) structures consisting of 2D alternating pathways for electronic charges and ionic species. These nanostructured materials act as efficient electrochromic redox systems that exhibit coupled electrochemical reduction and oxidation in the ordered bulk states. For example, compound **1** having the terthienylphenylcyanoethylene mesogen and the imidazolium triflate moiety forms the smectic LC nanostructure. Distinct reversible electrochromic responses are observed for compound **1** without additional electrolyte solution on the application of double-potential steps between 0 and 2.5 V in the smectic A phase at 160 °C. In contrast, compound **2** having a tetrafluorophenylterthiophene moiety and compound **3** having a phenylterthiophene moiety exhibit irreversible cathodic reduction and reversible anodic oxidation in the smectic A phases. The use of poly(3,4-ethylenedioxythiophene)−poly(4-styrene sulfonate) (PEDOT−PSS) as an electron-accepting layer on the cathode leads to the distinct electrochromic responses for **2** and **3**. These results show that new self-organized molecular redox systems can be built by nanosegregated π-conjugated liquid crystals containing imidazolium moieties with and without electroactive thin layers on the electrodes.

Introduction

The integration of molecular functions in supramolecular assemblies is a promising approach to the development of new materials exhibiting enhanced and dynamic functions.[1] Self-organized nanomaterials that exhibit electronic and ionic functions can be obtained by using liquid-crystalline (LC) molecular assemblies of π-conjugated and ionic molecular components.[2−4] Liquid crystals consisting of the ionic and nonionic moieties self-assemble into the nanosegregated structures such as columnar (cylinder),[3a−c,g,i] smectic (layer),[3d,e] and bicontinuous cubic[3f] phases to form anisotropic ion-conductive pathways. Efficient and anisotropic ionic conductions have been observed in these nanostructured LC phases.[3] Liquid crystals bearing π-conjugated moieties exhibit electronic charge transport[4] in the columnar[4f−i,n,o] and smectic phases.[4j−m] The enhanced transport properties of the electronic charge carriers for these

[†] The University of Tokyo.
[‡] Tokyo University of Agriculture and Technology.

(1) (a) Thomas, S. W., III; Joly, G. D.; Swager, T. M. *Chem. Rev.* **2007**, *107*, 1339–1386. (b) Jenekhe, S. A. *Nat. Mater.* **2008**, *7*, 354–355. (c) Comoretto, D. In *Supramolecular Polymers*, 2nd ed.; Ciferri, A., Ed; Taylor and Francis: London, 2005; p 509. (d) Leger, J. M. *Adv. Mater.* **2008**, *20*, 837–841. (e) Zhang, W.; Nuckolls, C. In *Supramolecular Polymers*, 2nd ed.; Ciferri, A., Ed; Taylor and Francis: London, 2005; p 751. (f) Thompson, B. C.; Fréchet, J. M. J. *Angew. Chem., Int. Ed.* **2008**, *47*, 58–77. (g) Hoeben, F. J. M.; Jonkheijm, P.; Meijer, E. W.; Schenning, A. P. H. J. *Chem. Rev.* **2005**, *105*, 1491–1546. (h) Fox, J. D.; Rowan, S. J. *Macromolecules* **2009**, *42*, 6823–6835. (i) Tsao, H. N.; Räder, H. J.; Pisula, W.; Rouhanipour, A.; Müllen, K. *Phys. Status Solidi A* **2008**, *205*, 421–429. (j) Deschenaux, R.; Donnio, B.; Guillon, D. *New J. Chem.* **2007**, *31*, 1064–1073. (k) Saez, I. M.; Goodby, J. W. *Struct. Bonding (Berlin)* **2008**, *128*, 1–62. (l) Nolte, R. J. M. *Liq. Cryst.* **2006**, *33*, 1373–1377. (m) Kato, T. *Science* **2002**, *295*, 2414–2418. (n) Kato, T.; Mizoshita, N.; Kishimoto, K. *Angew. Chem., Int. Ed.* **2006**, *45*, 38–68.

(2) (a) Funahashi, M.; Shimura, H.; Yoshio, M.; Kato, T. *Struct. Bonding (Berlin)* **2008**, *128*, 151–179. (b) Yazaki, S.; Funahashi, M.; Kato, T. *J. Am. Chem. Soc.* **2008**, *130*, 13206–13207. (c) Kerr, R. L.; Miller, S. A.; Shoemaker, R. K.; Elliot, B. J.; Gin, D. L. *J. Am. Chem. Soc.* **2009**, *131*, 15972–15973. (d) Pal, S. K.; Kumar, S. *Tetrahedron Lett.* **2006**, *47*, 8993–8997. (e) Motoyanagi, J.; Fukushima, T.; Aida, T. *Chem. Commun.* **2005**, 101–103. (f) El Hamaoui, B.; Zhi, L.; Pisula, W.; Kolb, U.; Wu, J.; Müllen, K. *Chem. Commun.* **2007**, 2384–2386. (g) Yasuda, T.; Tanabe, K.; Tsuji, T.; Coti, K. K.; Aprahamian, I.; Stoddart, J. F.; Kato, T. *Chem. Commun.* **2010**, *46*, 1224–1226.

(3) (a) Yoshio, M.; Mukai, T.; Ohno, H.; Kato, T. *J. Am. Chem. Soc.* **2004**, *126*, 994–995. (b) Shimura, H.; Yoshio, M.; Hoshino, K.; Mukai, T.; Ohno, H.; Kato, T. *J. Am. Chem. Soc.* **2008**, *130*, 1759–1765. (c) Yoshio, M.; Kagata, T.; Hoshino, K.; Mukai, T.; Ohno, H.; Kato, T. *J. Am. Chem. Soc.* **2006**, *128*, 5570–5577. (d) Hoshino, K.; Yoshio, M.; Mukai, T.; Kishimoto, K.; Ohno, H.; Kato, T. *J. Polym. Sci., Part A: Polym. Chem.* **2003**, *41*, 3486–3492. (e) Yoshio, M.; Mukai, T.; Kanie, K.; Yoshizawa, M.; Ohno, H.; Kato, T. *Adv. Mater.* **2002**, *14*, 351–354. (f) Ichikawa, T.; Yoshio, M.; Hamasaki, A.; Mukai, T.; Ohno, H.; Kato, T. *J. Am. Chem. Soc.* **2007**, *129*, 10662–10663. (g) Yoshio, M.; Ichikawa, T.; Shimura, H.; Kagata, T.; Hamasaki, A.; Mukai, T.; Ohno, H.; Kato, T. *Bull. Chem. Soc. Jpn.* **2007**, *9*, 1836–1841. (h) Yazaki, S.; Kamikawa, Y.; Yoshio, M.; Hamasaki, A.; Mukai, T.; Ohno, H.; Kato, T. *Chem. Lett.* **2008**, *37*, 538–539. (i) Shimura, H.; Yoshio, M.; Hamasaki, A.; Mukai, T.; Ohno, H.; Kato, T. *Adv. Mater.* **2009**, *21*, 1591–1594.

 10.1021/ja101366x

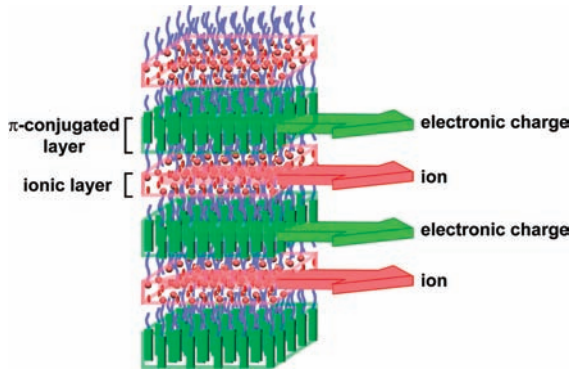

Figure 1. Schematic illustration of a nanostructured smectic LC phase for the coupling of the ionic and electronic functions.

liquid crystals have been applied to field-effect transistors[5a−h] and electroluminescence devices.[5i−k]

Our intention is to develop new redox-active materials by the combination of ionic and electronic functions in the nanostructured LC phases (Figure 1). We expect that the enhanced transportations of ions and electronic charge carriers couple in the nanosesegregated LC structures to produce new functional materials.[2b,6] In the present paper, we report on the efficient redox materials based on liquid crystals **1**−**3** (Figure 2). These molecules consist of π-conjugated mesogens and ionic moieties. They have been designed to induce smectic A (SmA) phases where the ion and hole transport layers are alternately formed through the nanosegregation. A new redox system is also designed by combining poly(3,4-ethylenedioxythiophene)−poly(4-styrene sulfonate) (PEDOT−PSS)[7] films with the liquid crystals.

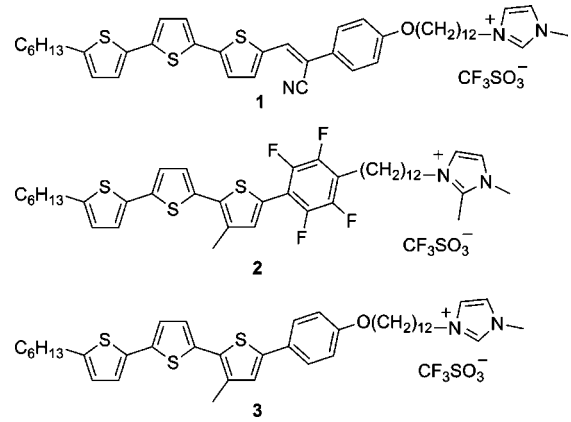

Figure 2. Molecular structures of liquid crystals **1**−**3**.

Conventional organic redox-active materials applied to electrochromic devices,[8] actuators,[9] and light-emitting electrochemical cells,[10] have been used as thin films dipped in electrolyte solutions or combined with solid electrolytes. Recently, we reported the preliminary results of the redox

(4) (a) O'Neill, M.; Kelly, S. M. *Adv. Mater.* **2003**, *15*, 1135–1146. (b) Shimizu, Y.; Oikawa, K.; Nakayama, K.; Guillon, D. *J. Mater. Chem.* **2007**, *17*, 4223–4229. (c) Sergeyev, S.; Pisula, W.; Geerts, Y. H. *Chem. Soc. Rev.* **2007**, *36*, 1902–1929. (d) Laschat, S.; Baro, A.; Steinke, N.; Giesselmann, F.; Hägele, C.; Scalia, G.; Judele, R.; Kapatsina, E.; Sauer, S.; Schreivogel, A.; Tosoni, M. *Angew. Chem., Int. Ed.* **2007**, *46*, 4832–4887. (e) Pisula, W.; Zorn, M.; Chang, J. Y.; Müllen, K.; Zentel, R. *Macromol. Rapid Commun.* **2009**, *30*, 1179–1202. (f) Boden, N.; Bushby, R. J.; Clements, J.; Jesudason, M. V.; Knowles, P. F.; Williams, G. *Chem. Phys. Lett.* **1988**, *152*, 94–99. (g) Adam, D.; Closs, F.; Frey, T.; Funhoff, D.; Haarer, D.; Ringsdorf, H.; Schuhmacher, P.; Siemensmeyer, K. *Phys. Rev. Lett.* **1993**, *70*, 457–460. (h) van de Craats, A. M.; Warman, J. M.; Fechtenkötter, A.; Brand, J. D.; Harbison, M. A.; Müllen, K. *Adv. Mater.* **1999**, *11*, 1469–1472. (i) Breiby, D. W.; Bunk, O.; Pisula, W.; Sølling, T. I.; Tracz, A.; Pakula, T.; Müllen, K.; Nielsen, M. M. *J. Am. Chem. Soc.* **2005**, *127*, 11288–11293. (j) Funahashi, M.; Hanna, J. *Appl. Phys. Lett.* **2000**, *76*, 2574–2576. (k) Funahashi, M.; Hanna, J. *Adv. Mater.* **2005**, *17*, 594–598. (l) Prehm, M.; Götz, G.; Bäuerle, P.; Liu, F.; Zeng, X.; Ungar, G.; Tschierske, C. *Angew. Chem., Int. Ed.* **2007**, *46*, 7856–7859. (m) Apperloo, J. J.; Janssen, R. A. J.; Malenfant, P. R. L.; Groenendaal, L.; Fréchet, J. M. J. *J. Am. Chem. Soc.* **2000**, *122*, 7042–7051. (n) Yasuda, T.; Kishimoto, K.; Kato, T. *Chem. Commun.* **2006**, 3399–3401. (o) Yasuda, T.; Ooi, H.; Morita, J.; Akama, Y.; Minoura, K.; Funahashi, M.; Shimomura, T.; Kato, T. *Adv. Funct. Mater.* **2009**, *19*, 411–419.

(5) (a) Funahashi, M. *Polym. J.* **2009**, *41*, 459–469. (b) Funahashi, M.; Zhang, F.; Tamaoki, N. *Adv. Mater.* **2007**, *19*, 353–358. (c) Zhang, F.; Funahashi, M.; Tamaoki, N. *Org. Electron.* **2009**, *10*, 73–84. (d) Garnier, F.; Hajlaoui, R.; El Kassmi, A.; Horowitz, G.; Laigre, L.; Porzio, W.; Armanini, M.; Provasoli, F. *Chem. Mater.* **1998**, *10*, 3334–3339. (e) Oikawa, K.; Monobe, H.; Nakayama, K.; Kimoto, T.; Tsuchiya, K.; Heinrich, B.; Guillon, D.; Shimizu, Y.; Yokoyama, M. *Adv. Mater.* **2007**, *19*, 1864–1868. (f) van Breemen, A. J. J. M.; Herwig, P. T.; Chlon, C. H. T.; Sweelssen, J.; Schoo, H. F. M.; Setayesh, S.; Hardeman, W. M.; Martin, C. A.; de Leeuw, D. M.; Valeton, J. J. P.; Bastiaansen, C. W. M.; Broer, D. J.; Popa-Merticaru, A. R.; Meskers, S. C. J. *J. Am. Chem. Soc.* **2006**, *128*, 2336–2345. (g) van de Craats, A. M.; Stutzmann, N.; Bunk, O.; Nielsen, M. M.; Watson, M.; Müllen, K.; Chanzy, H. D.; Sirringhaus, H.; Friend, R. H. *Adv. Mater.* **2003**, *15*, 495–499. (h) Pisula, W.; Menon, A.; Stepputat, M.; Lieberwirth, I.; Kolb, U.; Tracz, A.; Sirringhaus, H.; Pakula, T.; Müllen, K. *Adv. Mater.* **2005**, *17*, 684–689. (i) Contoret, A. E. A.; Farrar, S. R.; Jackson, P. O.; Khan, S. M.; May, L.; O'Neill, M.; Nicholls, J. E.; Kelly, S. M.; Richards, G. J. *Adv. Mater.* **2000**, *12*, 971–974. (j) Aldred, M. P.; Contoret, A. E. A.; Farrar, S. R.; Kelly, S. M.; Mathieson, D.; O'Neill, M.; Tsoi, W. C.; Vlachos, P. *Adv. Mater.* **2005**, *17*, 1368–1372. (k) Kogo, K.; Goda, T.; Funahashi, M.; Hanna, J. *Appl. Phys. Lett.* **1998**, *73*, 1595–1597.

(6) (a) Tabushi, I.; Yamamura, K.; Kominami, K. *J. Am. Chem. Soc.* **1986**, *108*, 6409–6410. (b) Tanabe, K.; Yasuda, T.; Yoshio, M.; Kato, T. *Org. Lett.* **2007**, *9*, 4271–4274. (c) Suisse, J.-M.; Douce, L.; Bellemin-Laponnaz, S.; Maisse-François, A.; Welter, R.; Miyake, Y.; Shimizu, Y. *Eur. J. Inorg. Chem.* **2007**, 3899–3905. (d) Aprahamian, I.; Yasuda, T.; Ikeda, T.; Saha, S.; Dichtel, W. R.; Isoda, K.; Kato, T.; Stoddart, J. F. *Angew. Chem., Int. Ed.* **2007**, *46*, 4675–4679. (e) Chang, H.-C.; Shiozaki, T.; Kamata, A.; Kishida, K.; Ohmori, T.; Kiriya, D.; Yamauchi, T.; Furukawa, H.; Kitagawa, S. *J. Mater. Chem.* **2007**, *17*, 4136–4138.

(7) (a) Groenendaal, L. B.; Jonas, F.; Freitag, D.; Pielartzik, H.; Reynolds, J. R. *Adv. Mater.* **2000**, *12*, 481–494. (b) Greczynski, G.; Kugler, T.; Keil, M.; Osikowicz, W.; Fahlman, M.; Salaneck, W. R. *J. Electron Spectrosc. Relat. Phenom.* **2001**, *121*, 1–17. (c) Ko, H. C.; Kang, M.; Moon, B.; Lee, H. *Adv. Mater.* **2004**, *16*, 1712–1716.

(8) (a) Mortimer, R. J.; Dyer, A. L.; Reynolds, J. R. *Displays* **2006**, *27*, 2–18. (b) Onoda, M.; Nakayama, H.; Morita, S.; Yoshino, K. *J. Appl. Phys.* **1993**, *73*, 2859–2865. (c) Liou, G.-S.; Chang, C.-W. *Macromolecules* **2008**, *41*, 1667–1674. (d) Wu, C.-G.; Lu, M.-I.; Chang, S.-J.; Wei, C.-S. *Adv. Funct. Mater* **2007**, *17*, 1063–1070. (e) Lu, W.; Fadeev, A. G.; Qi, B.; Smela, E.; Mattes, B. R.; Ding, J.; Spinks, G. M.; Mazurkiewicz, J.; Zhou, D.; Wallace, G. G.; MacFarlane, D. R.; Forsyth, S. A.; Forsyth, M. *Science* **2002**, *297*, 983–987. (f) Argun, A. A.; Cirpan, A.; Reynolds, J. R. *Adv. Mater.* **2003**, *15*, 1338–1341. (g) Sapp, S. A.; Sotzing, G. A.; Reynolds, J. R. *Chem. Mater.* **1998**, *10*, 2101–2108. (h) Sapp, S. A.; Sotzing, G. A.; Reddinger, J. L.; Reynolds, J. R. *Adv. Mater.* **1996**, *8*, 808–811. (i) Cutler, C. A.; Bouguettaya, M.; Reynolds, J. R. *Adv. Mater.* **2002**, *14*, 684–688.

(9) (a) Smela, E. *Adv. Mater.* **2003**, *15*, 481–494. (b) Baughman, R. H. *Synth. Met.* **1996**, *78*, 339–353. (c) Jager, E. W. H.; Smela, E.; Inganäs, O. *Science* **2000**, *290*, 1540–1545. (d) Carpi, F.; Gallone, G.; Galantini, F.; De Rossi, D. *Adv. Funct. Mater.* **2008**, *18*, 235–241.

(10) (a) Pei, Q.; Yu, G.; Zhang, C.; Yang, Y.; Heeger, A. J. *Science* **1995**, *269*, 1086–1088. (b) Shao, Y.; Bazan, G. C.; Heeger, A. J. *Adv. Mater.* **2007**, *19*, 365–370. (c) Slinker, J. D.; DeFranco, J. A.; Jaquith, M. J.; Silveira, W. R.; Zhong, Y.-W.; Moran-Mirabal, J. M.; Craighead, H. G.; Abruña, H. D.; Marohn, J. A.; Malliaras, G. G. *Nat. Mater.* **2007**, *6*, 894–899. (d) Fang, J.; Matyba, P.; Robinson, N. D.; Edman, L. *J. Am. Chem. Soc.* **2008**, *130*, 4562–4568. (e) Shin, J.-H.; Edman, L. *J. Am. Chem. Soc.* **2006**, *128*, 15568–15569. (f) Matyba, P.; Maturova, K.; Kemerink, M.; Robinson, N. D.; Edman, L. *Nat. Mater.* **2009**, *8*, 672–676.

Scheme 1. Synthetic Routes of Liquid Crystals **1** and **2**

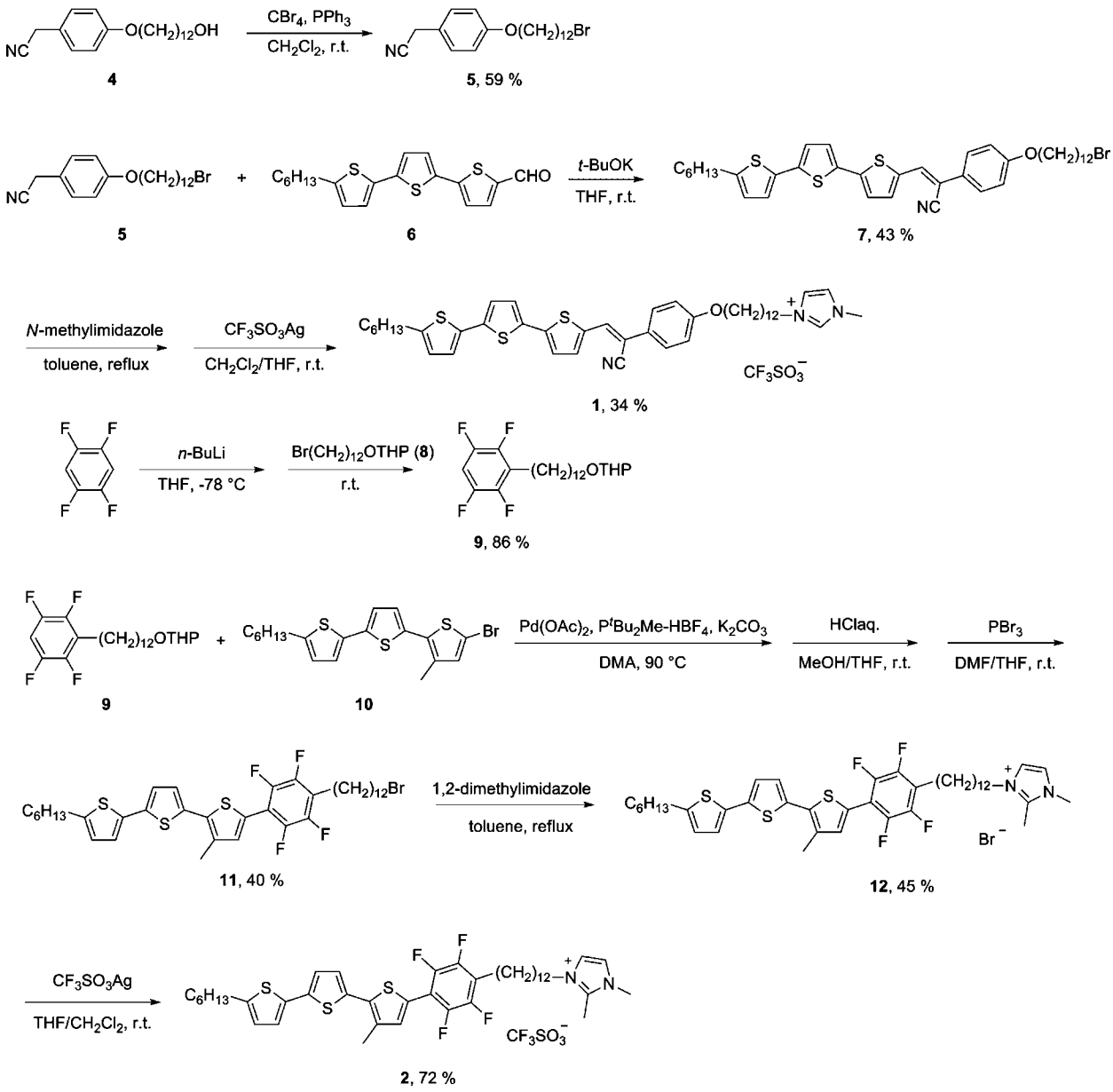

behavior for compound **3** in the LC phase without electrolytes (Figure 2).[2b] The ion and hole transportations in the nanostructured SmA phase induced electrochromism without electrolytes.

In the redox activity of the liquid crystals combining ionic and electronic functions, the mobile ions in the nanostructure play a crucial role. The enhancement of electronic functions by the combination with ions has been studied in conjugated polyelectrolytes.[11] The conjugated polyelectrolytes consisting of π-conjugated polymer backbones bearing ionic moieties have been applied to light-emitting diodes,[11a,b] light-emitting electrochemical cells,[11c−g] and solar cells.[11h,i] However, the electronic charge carrier mobilities are low, of the order of 10^{-7}−10^{-6} cm^2 V^{-1} s^{-1}, because of the disordered structures of the polymers.[11c] Their ionic conductivities are also low because of the large viscosity. In contrast, the efficient ion and hole transports are possible in the nanosegregated smectic liquid crystals where the structure of ion- and hole-transporting layers is well-defined on the scale of nanometer.

Results and Discussion

Synthesis of Materials. Compounds **1** and **2** were synthesized as shown in Scheme 1. The Knoevenagel condensation between 4-(12-bromododecyloxyphenyl)acetonitrile (**5**) and 5-hexyl-2,2′:5′,2″-terthiophene-5″-carbaldehyde (**6**) yielded cyanoethylene derivative **7**. The quaternization reaction of *N*-methylimidazole with compound **7** followed by anion exchange using silver triflate afforded liquid crystal **1**. The aromatic core of compound **2** was synthesized by the Pd(0)-catalyzed coupling reaction[5c,12] between tetrafluorobenzene derivative **9** and 5-bromo-2′-hexyl-2,2′:5′,2″-terthiophene derivative **10**. The transformation from the intermediate **11** to compound **2** was carried out by a procedure similar to that for compound **3**.[2b]

Mesomorphic Behavior. The LC properties of **1**−**3** are summarized in Table 1. Compounds **1**−**3** exhibit the enantio-

Table 1. Thermal Properties of Liquid Crystals **1**−**3**

compd	thermal properties[a]				
1	Cr	79 (18)	SmA	185 (7.7)	Iso
2	Cr	75 (16)	SmA	149 (2.7)	Iso
3	Cr	90 (48)	SmA	152 (4.3)	Iso

[a] Transition temperatures (°C) are given as the onset of the peaks detected by the differential scanning calorimetry (DSC) measurements on the second heating at a scanning rate of 10 °C min^{-1}. The transition enthalpies (kJ mol^{-1}) are in parentheses. Cr: crystalline. SmA: smectic A. Iso: isotropic liquid. For liquid crystals **2**, the transition peaks corresponding to the crystallization and melting are observed below the Cr−SmA transition temperature on the heating cycle in the DSC thermogram (see Supporting Information).

tropic smectic A (SmA) phases. The focal-conic fan textures are observed by the polarizing microscope observation for **1** and **2** on polyimide films in the mesomorphic temperature ranges (Figure 3). On glass substrates, the homeotropic textures for **1** and **2** are observed as dark fields.

The LC structures of **1**−**3** have been studied by small-angle X-ray scattering (see Supporting Information, Figure S5) and wide-angle X-ray diffraction. The wide-angle X-ray diffraction patterns for compounds **1** and **2** in the SmA phases show two diffraction peaks indexed as (002) and (003) in the low angle regions, indicating a layer spacing of 51 Å for compound **1** at 160 °C (Figure 4) and a layer spacing of 51 Å for **2** at 120 °C (see Supporting Information). In small-angle X-ray scattering patterns for compounds **1** and **2**, weak peaks corresponding to (001) diffractions are observed (see Supporting Information). No peaks are observed in the wide-angle regions for **1** and **2** other than the diffusive halo. The molecular lengths of **1** and **2** are estimated to be approximately 47 and 45 Å, respectively, by molecular mechanics (MM2) calculations. The results indicate that the LC molecules are arranged in the smectic layers in the antiparallel manner as shown in Figure 5.[13] The nanosegregation leads to the formation of the LC nanostructures in which two-dimensional layers of the π-conjugated mesogens and ionic moieties are separatedly self-organized by the insulating alkyl chains. The formation of such a layered nanostructure was also observed for compound **3** in the SmA phase as reported in our previous communication.[2b]

Redox Properties in Solution States. The redox properties of compounds **1**−**3** in the CH_2Cl_2 solution states have been examined by the cyclic voltammetry measurement (Figure 6). For compound **1**, quasi-reversible one-electron oxidation and one-electron reduction are observed at the half-wave potentials of 0.86 and −1.62 V versus Ag^+/Ag, respectively (Figure 6a). The cyclic voltammograms of compounds **2** and **3** (Figure 6b,c) exhibit only quasi-reversible one-electron oxidations without any reversible reduction peaks within the electrochemical window of the electrolyte solution. The oxidation peaks of **2** and **3** are observed at the half-wave potentials of 0.98 and 0.69 V versus Ag^+/Ag, respectively. For compound **1**, the electron-withdrawing cyano group effectively stabilizes the reduced anionic state,[14] leading to the quasi-reversible electrochemical reduction besides the quasi-reversible oxidation. The tetrafluorophenyl group of **2** also withdraws electrons, leading to an increase in the oxidation potential. However, the radical anion state of the π-conjugated system of **2** is not sufficiently stabilized, resulting in the irreversible reduction. These results show that compound **1** has a suitable mesogen that could be used in the electrochromism in the LC state.

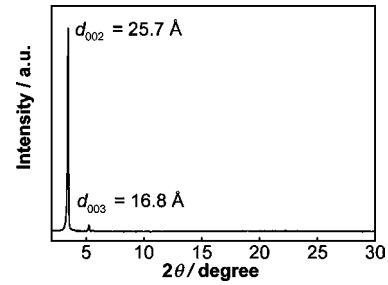

Figure 4. X-ray diffraction pattern for **1** in the SmA phase at 160 °C.

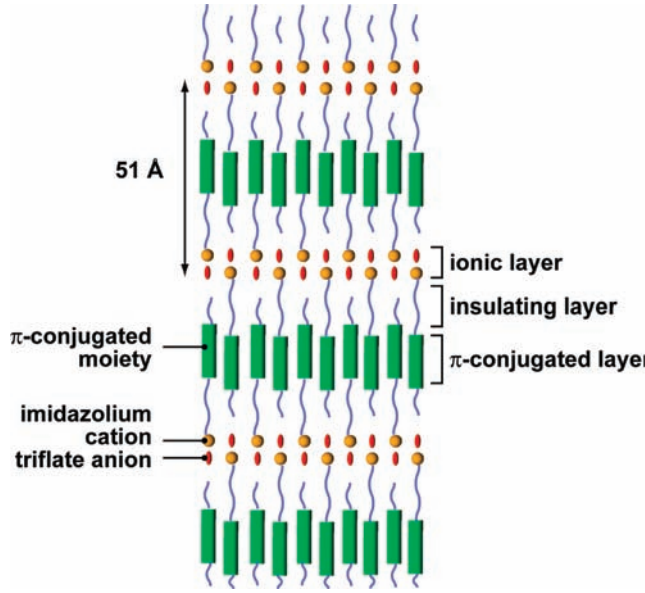

Figure 5. Schematic illustration of a possible structure in the SmA phases for liquid crystals **1**−**3**. Green cylinders, red ellipsoids, and orange spheres represent π-conjugated moieties, triflate anions, and imidazolium cations, respectively. The ionic and π-conjugated moieties are organized into segregated layers.

Redox Activities in the Bulk States. The redox responses of liquid crystals **1**−**3** in the bulk states have been achieved. The response behavior was measured by monitoring the transmitted light intensity of a He−Ne laser (λ = 632.8 nm) through the

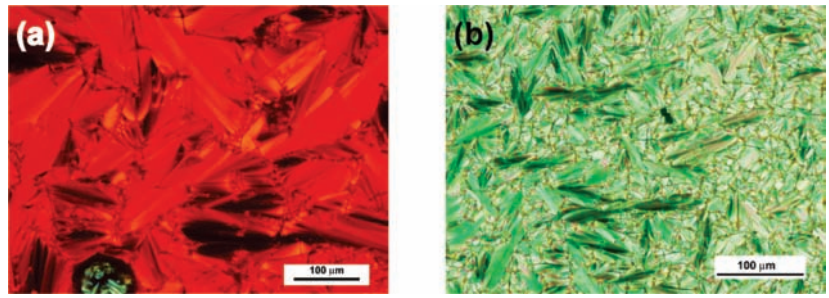

Figure 3. Polarizing optical photomicrographs of liquid crystals: **1** (a) and **2** (b) at 120 °C.

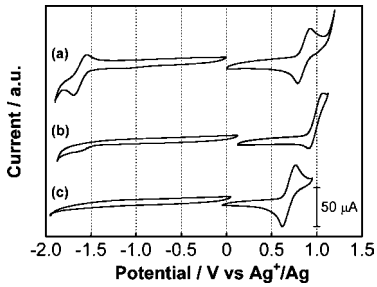

Figure 6. Cyclic voltammograms of the CH_2Cl_2 solutions of compounds **1** (a), **2** (b), and **3** (c) (2.0 mM) with a Pt working electrode. The supporting electrolyte is Bu_4NClO_4 (0.10 M). The sweep rate is 100 mV s^{-1} except for the negative potential region of compound **2**, where the rate is 50 mV s^{-1}.

samples of **1**−**3** in the cells consisting of two ITO-coated glass plates. The ITO electrodes were coated with polyimide thin films to deactivate the surface defects on the ITO.[15] The polyimide thin films preserve the conductivities of the ITO surface.[5k] The cells were filled with the compounds in the isotropic states by capillary action. When the samples were cooled to the SmA phases, focal-conic fan textures were observed by using a polarizing optical microscope, indicating that the LC molecules were aligned parallel to the electrode surfaces. In those alignments, the smectic layers were vertical to the electrode surfaces and the electric fields were applied in the direction of the ion transport layers. Figure 7 shows the responses of the transmittance for compounds **1** and **3** in the liquid crystal cells as a function of time on the application of double-potential steps between 0 and 2.5 V. The responses of the transmittance observed for compound **1** (Figure 7a) are more distinct than those for **3** (Figure 7b). The value of the driving voltage of 2.5 V for **1** is close to its HOMO−LUMO energy gap of 2.4 V (see Supporting Information, Figure S2). This observation suggests that the electrochemical oxidation at the anode couples with the reduction at the cathode in the SmA phase of compound **1**, as shown in Figure 8a. In contrast, the change of the transmittance for compound **3** is almost negligible on the application of the same potential steps between 0 and 2.5 V (Figure 7b). The increased applied voltage of 5 V is required to give a clear color change for liquid crystal **3** as was observed in our preliminary experiment.[2b] The value of the HOMO−LUMO energy gap for **3** is 2.8 eV (see Supporting Information, Figure S2). The driving voltage for **3**, which is 2.2 V higher than its HOMO−LUMO energy gap, can be ascribed to the irreversible cathodic reduction of compound **3**, although the oxidation process of **3** at the anode is reversible (Figure 8b). After repeated redox cycles, decomposed red products are observed on the cathode of the cell for liquid crystal **3**. For liquid crystal **2** containing the tetrafluorophenyl moiety, no color change is observed on the application of the double-potential steps between 0 and 2.5 V in the SmA phase. When the applied voltage is increased to 5 V, the color slightly changes. The irreversible cathodic reduction and the high oxidation potential for liquid crystal **2** (Figure 6b) result in the unstable electrochromic behavior.

Liquid crystal **3** was expected to exhibit efficient electrochromic responses if the anodic oxidation is coupled with the

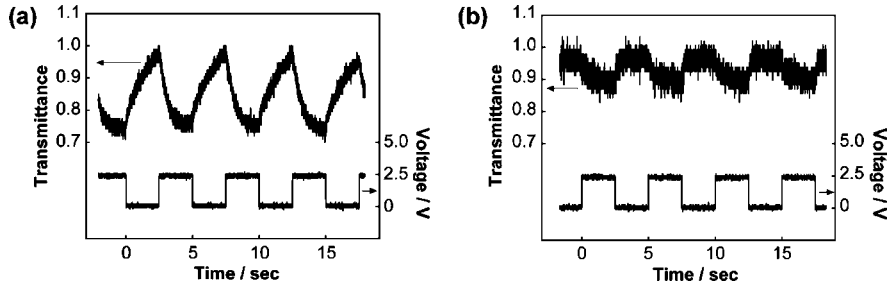

Figure 7. Responses of transmittance of the cell with compound **1** in the SmA phase at 160 °C (a) and with compound **3** in the SmA phase at 120 °C (b) on the application of double-potential steps between 0 V (2.5 s) and 2.5 V (2.5 s). The sample thickness is 4 μm.

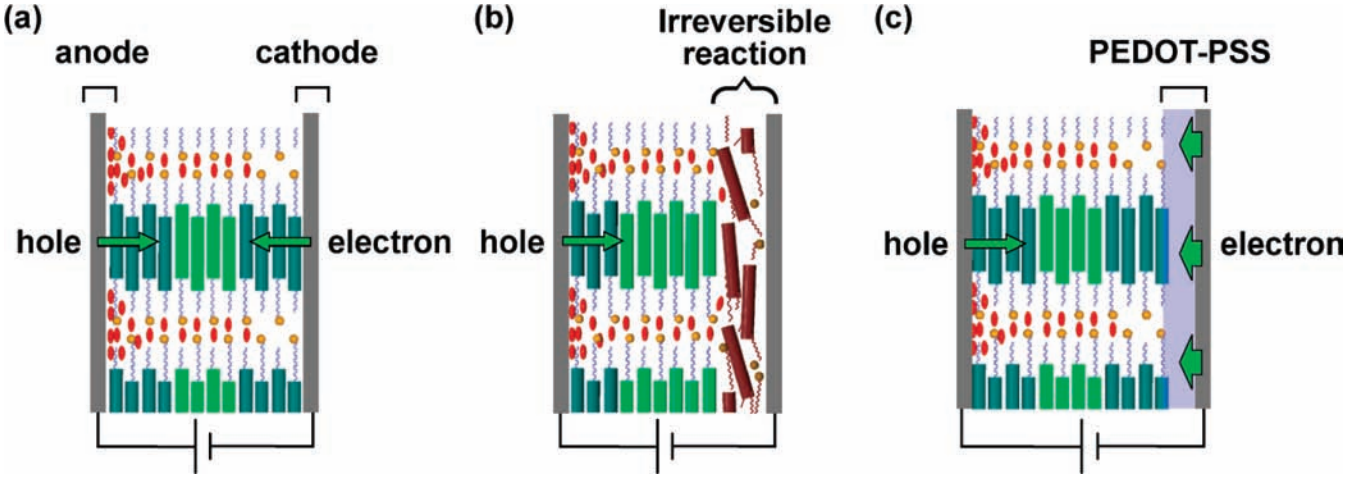

Figure 8. Schematic illustration of the redox molecular systems combining ionic and electronic functions. (a) The redox system of liquid crystal **1** exhibiting reversible reduction besides the reversible oxidation. (b) The redox system of liquid crystal **3** whose anion radical state is not stabilized. The cathodic reduction is irreversible, while the anodic oxidation is reversible. (c) The redox system of liquid crystal **3** using the PEDOT−PSS thin film as an electron acceptor coated on the cathode combined with the reversible oxidation of liquid crystal **3**. The light-green cylinders represent neutral π-conjugated moieties. The dark-green cylinders are the oxidized or reduced ones. The red ellipsoids and orange spheres represent triflate anions and imidazolium cations, respectively. The brown cylinders in (b) represent decomposed products of liquid crystal **3** by the irreversible reduction.

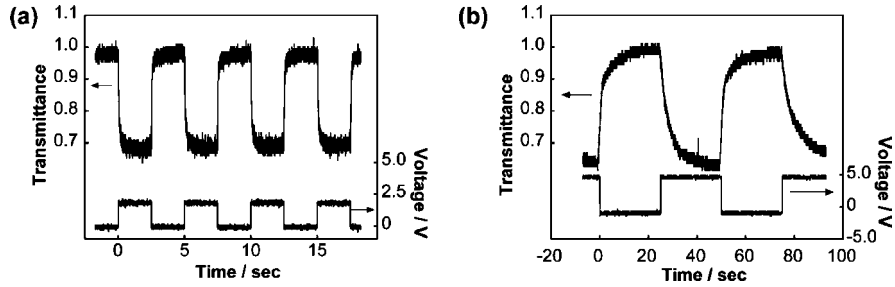

Figure 9. Responses of the transmittance of the cell with compound **3** in the SmA phase at 120 °C. (a) The double-potential steps between 0 V (2.5 s) and 2 V (2.5 s) are applied to the cell. The cathode and the anode of the cell are coated with PEDOT−PSS and polyimide, respectively. The sample thickness is 7 μm. (b) The double-potential steps between −1 V (25 s) and 5 V (25 s) are applied to the cell. The cathode and anode of the cell are bare ITO electrodes. The sample thickness is 4 μm.

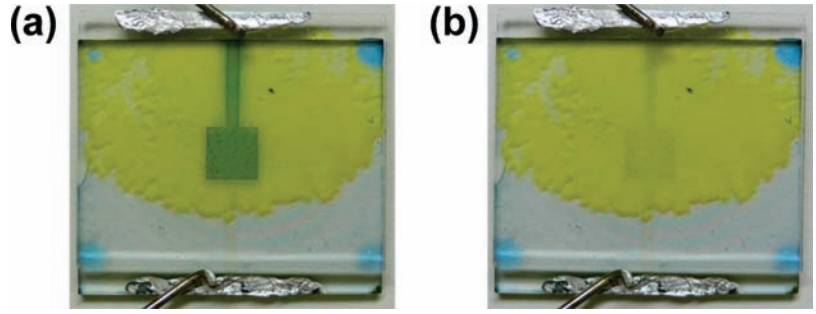

Figure 10. Photographs of the cell for compound **3** in the SmA phase at 120 °C at the applied potential of 2 V (a) and 0 V (b). In the cell, the cathode and the anode are coated with PEDOT−PSS and polyimide films, respectively. The sample thickness is 7 μm.

cathodic reduction as schematically illustrated in Figure 8c. The PEDOT−PSS layer has been chosen as an electron acceptor on the cathode for the combination with liquid crystal **3**. On the anode, the electrons released from the π-conjugated systems of liquid crystal **3** should be compensated rapidly by the electron acceptance on the cathodic PEDOT−PSS layer (Figure 8c). Figure 9a shows the responses of the transmittance under the double-potential application between 0 and 2 V for compound **3** in the ITO cell whose cathode is spin-coated with the PEDOT−PSS thin film. The distinct responses are observed under the application of a potential of only 2 V. The fast switching of the order of several hundred milliseconds is observed in Figure 9a. Figure 9b shows the responses for **3** sandwiched between bare ITO electrodes under the double-potential application between −1 and 5 V, where the response time is about several seconds.[2b] The driving voltage (Figure 9a) is reduced as a consequence of the lower reduction voltage for PEDOT−PSS compared with that for compound **3**. These fast responses can be attributed to the fast cathodic reduction of the PEDOT−PSS film coupled with the fast anodic oxidation of **3**. The deactivation of the defects on the ITO anode surface by the polyimide coating may also contribute to the improvement in the electrochromic behavior. Figures 10 presents the photographs of the liquid crystal cell whose cathode is coated with the PEDOT−PSS film for compound **3** in the SmA phase at 120 °C. The clear change of color between pale yellow and dark blue is observed under the double-potential application between 0 and 2 V. For compound **2**, coating the cathode with the PEDOT−PSS thin film is also effective to improve the electrochromic response (data not shown).

Ionic Conductivities. The mobile ions should play a critical role in the electrochromic responses in the bulk nanosegregated states of compounds **1**−**3**. In fact, such electrochromism is not observed in the conventional LC semiconductors based on π-conjugated systems without ionic moieties or based on ionic liquid crystals without the π-conjugated chromophores.

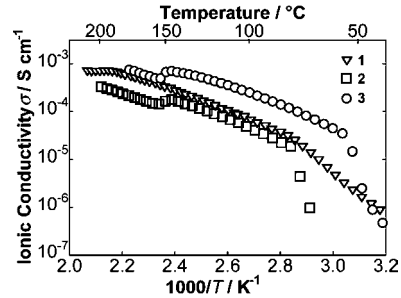

Figure 11. Ionic conductivities of **1**−**3** as a function of temperature.

The ionic conductivities of compounds **1**−**3** parallel to the smectic layers have been measured by the alternating current impedance method[16] using comb-shaped gold electrodes deposited on a glass substrate.[3] The samples were embedded between the electrodes on the substrate covered with another glass plate. The samples exhibit the homeotropic alignment on the glass substrates. The ionic conductivities of compounds **1**−**3** as a function of temperature are shown in Figure 11. The ionic conductivities are 4.7×10^{-4} S cm^{-1} for compound **1** at 160 °C, 1.2×10^{-4} S cm^{-1} for **2** at 130 °C, and 3.9×10^{-4} S cm^{-1} for **3** at 120 °C. These values are lower than those for electrolytes such as a mixture of poly(ethylene oxide) and lithium salts above 100 °C. However, they are comparable with those of nanosegregated ionic liquid crystals.[3] In the SmA phases of compounds **1**−**3**, effective ionic transport occurs along the smectic layers formed by the nanosegregation. Such self-organization behavior is not observed for conventional polyelectrolytes.[17] The ionic conductivities in the SmA phases of the liquid crystals **1**−**3** increase with the temperature because of the thermal activation process of the ionic transport. For compounds **2** and **3**, which exhibit isotropic−smectic transitions at around 150 °C, discontinuous increases in the conductivities are observed at the phase transitions. This behavior was observed for the columnar and smectic ionic liquid crystals.[3] After

crystallization, the ion conductivities decrease for **1**−**3**. For example, the ionic conductivities of **3** suddenly drop because of the crystallization at 57 °C. These results show that nanosegeregated layered smectic LC structures can be used for new electrolytes in functional materials.

Conclusion

The LC nanostructures consisting of the ion-conductive and electronic charge transport layers have been built by the association of π-conjugated molecules having ionic moieties. These liquid crystals **1**−**3** exhibit nanostructured SmA phases where high ionic conductivities are observed. The combination of the enhanced ion and electronic charge transports in the nanostructured LC phases has resulted in efficient electrochromism in the LC bulk states. The low driving voltage and the reversible electrochemical oxidation and reduction have been achieved for liquid crystal **1**, which forms stabilized cation and anion radicals. The electrochromic properties of the liquid crystals have been enhanced by using a PEDOT−PSS layer on the cathode as an electron-accepting layer. The combination of the ionic and electronic functions in the nanostructured LC phases should be effective in applications to various electronic devices such as light-emitting electrochemical cells and electrochromic devices. The present results show new strategy for the design of electroactive and ion-active materials.

Experimental Section

General Procedures. ^{1}H and ^{13}C NMR spectra were obtained using a JEOL JNM-LA400 at 400 and 100 MHz for $CDCl_3$ solutions, respectively. Chemical shifts of ^{1}H and ^{13}C NMR signals are quoted to Me_4Si ($\delta = 0.00$) and $CDCl_3$ ($\delta = 77.00$) as internal standards, respectively. IR measurements were conducted on a JASCO FT/IR-660 Plus spectrometer. Matrix-assisted laser desorption ionization time-of-flight (MALDI-TOF) mass spectra were recorded on an Applied Biosystems Voyager-DE STR spectrometer. Elemental analyses were carried out with a Yanaco MT-6 CHN autocorder. A polarizing microscope Olympus BX51 equipped with a Mettler FP82HT hot stage was used for visual observation of the optical textures. Differential scanning calorimetry (DSC) measurements were conducted with a NETZSCH DSC 204 Phoenix. X-ray diffraction (XRD) measurements were carried out on a Rigaku RINT 2500 diffractometer with a heating stage and with the use of Ni-filtered Cu Kα radiation.

Measurement of Ionic Conductivities. Temperature dependence of the ionic conductivities was measured in the cooling process by the alternating current impedance method using a Schlumberger Solartron 1260 impedance analyzer (frequency range of 10 Hz to 10 MHz, applied voltage of 0.3 V) equipped with a temperature controller. The cooling rate was fixed to 2 K min^{-1}. Ionic conductivities were practically calculated to be the product of $1/R_b$ (Ω^{-1}) times cell constants (cm^{-1}) of the comb-shaped gold electrodes, which were calibrated with KCl aqueous solution (1.00 mmol L^{-1}) as a standard conductive solution. The impedance data (Z) were modeled as a connection of two RC circuits in series.

Electrochemical Measurement for the Solutions. Cyclic voltammetry (CV) was performed using an ALS CHI 600B electrochemical analyzer and a three-electrode cell equipped with a Pt working electrode, a Pt counter electrode, and an Ag^+/Ag reference electrode. A solution of Bu_4NClO_4 in CH_2Cl_2 (0.10 M) was used as the supporting electrolyte. All the potentials were calibrated with an Fc^+/Fc couple using ferrocene as an internal reference. Spectroelectrochemical measurements were conducted on a JASCO V-670 spectrometer together with a potentiostat and a three-electrode cell using the same supporting electrolyte as that used for CV.

Electrochemical Measurement for the Bulk Liquid Crystals. A He−Ne laser (Melles Griot 05 LPL 479, wavelength 632.8 nm) was used as a light source to measure the transmittance through the liquid crystal cell on a hot stage. A photodiode, a serial resistor, a bipolar amplifier (HAS 4011), a function generator (WF 1943A), and a digital oscilloscope (Tektronics TDS 3044B) were used for the light detecting system. The measurements were carried out under atmospheric conditions. The liquid crystal cells comprised two glass plates coated with indium tin oxide (ITO) (the area of the electrode was 4 mm × 4 mm. The ITO electrodes were covered with a thin film of PEDOT−PSS or polyimide (JSR AL1254). The deposition of the PEDOT−PSS thin films on the ITO-coated glass plates was performed by spin-coating them with its dispersion (Aldrich, 1.3−1.7% in H_2O) at a rotation speed of 2000 rpm for 300 s, followed by drying them at 100 °C for 20 min. The thickness of the cell was calculated from the interference fringes in its absorption spectrum. The liquid crystals were capillary-filled into the cells in the isotropic states. The air dissolved in the liquid crystals was purged with argon in the isotropic state using a vacuum pump before the measurements. The intensity of the transmitted light through the liquid crystal cells on the application of potential steps was detected by the photodiode and recorded using the digital oscilloscope. The transmittance was determined as the ratio of the intensity of the transmitted light through the liquid crystal cell during the measurement to the intensity before the potential application. The potential steps were applied by the function generator and the amplifier.

Acknowledgment. This study was partially supported by Grant-in-Aid for Scientific Research (A) (Grant No. 19205017) from the Japan Society for the Promotion of Science (JSPS) and the Global COE Program for Chemistry Innovation through Cooperation of Science and Engineering from the Ministry of Education, Culture, Sports, Science and Technology. S.Y. is thankful for financial support from JSPS Research Fellowships for Young Scientists. The authors are grateful to JSR Corporation for supplying the material forming the polyimide layers.

Supporting Information Available: Synthesis of **1** and **2**, DSC thermograms of **1** and **2**, UV−vis absorption spectra of **1**−**3**, UV−vis−NIR absorption spectra of **1** and **2** under the oxidation and reduction potentials, wide-angle X-ray diffraction pattern of **2**, and small-angle X-ray diffraction patterns of **1** and **2**. This material is available free of charge via the Internet at http://pubs.acs.org.

JA101366X

(11) (a) Yang, R.; Xu, Y.; Dang, X.-D.; Nguyen, T.-Q.; Cao, Y.; Bazan, G. C. *J. Am. Chem. Soc.* **2008**, *130*, 3282–3283. (b) Hoven, C.; Yang, R.; Garcia, A.; Heeger, A. J.; Nguyen, T.-Q.; Bazan, G. C. *J. Am. Chem. Soc.* **2007**, *129*, 10976–10977. (c) Hoven, C. V.; Garcia, A.; Bazan, G. C.; Nguyen, T.-Q. *Adv. Mater.* **2008**, *20*, 3793–3810. (d) Hodgkiss, J. M.; Tu, G.; Albert-Seifried, S.; Huck, W. T. S.; Friend, R. H. *J. Am. Chem. Soc.* **2009**, *131*, 8913–8921. (e) Edman, L.; Pauchard, M.; Liu, B.; Bazan, G.; Moses, D.; Heeger, A. J. *Appl. Phys. Lett.* **2003**, *82*, 3961–3963. (f) Ortony, J. H.; Yang, R.; Brzezinski, J. Z.; Edman, L.; Nguyen, T.-Q.; Bazan, G. C. *Adv. Mater.* **2008**, *20*, 298–302. (g) Hohertz, D.; Gao, J. *Adv. Mater.* **2008**, *20*, 3298–3302. (h) Qiao, Q.; Su, L.; Beck, J.; McLeskey, J. T., Jr. *J. Appl. Phys.* **2005**, *98*, 094906. (i) Yang, J.; Garcia, A.; Nguyen, T.-Q. *Appl. Phys. Lett.* **2007**, *90*, 103514.
(12) Lafrance, M.; Rowley, C. N.; Woo, T. K.; Fagnou, K. *J. Am. Chem. Soc.* **2006**, *128*, 8754–8756.
(13) (a) Mathevet, F.; Masson, P.; Nicoud, J.-F.; Skoulios, A. *Chem.−Eur. J.* **2002**, *8*, 2248–2254. (b) Abdallah, D. J.; Lu, L.; Cocker, T. M.; Bachman, R. E.; Weiss, R. G. *Liq. Cryst.* **2000**, *27*, 831–837.
(14) Ho, H. A.; Brisset, H.; Elandaloussi, E. H.; Frère, P.; Roncali, J. *Adv. Mater.* **1996**, *8*, 990–994.
(15) Huang, Z. H.; Zeng, X. T.; Sun, X. Y.; Kang, E. T.; Fuh, J. Y. H.; Lu, L. *Thin Solid Films* **2009**, *517*, 4810–4813.
(16) Macdonald, J. R. *Impedance Spectroscopy Emphasizing Solid Materials and Systems*; John Wiley & Sons: New York, 1987.
(17) Meyer, W. H. *Adv. Mater.* **1998**, *10*, 439–448.